

ANDALUSITE FORMATION IN A FAST EXHUMING HIGH-P WEDGE: TEXTURAL, MICROCHEMICAL, AND SM-ND AND Rb-Sr AGE CONSTRAINTS FOR A CRETACEOUS P-T-t PATH AT KIENBERG, SAUALPE (EASTERN ALPS)

Martin THÖNI¹⁾ & Christine MILLER²⁾

KEYWORDS

decompression melting
garnet Sm-Nd dating
Eoalpine event
P-T-t path
andalusite
Sausalpe

¹⁾ Department für Lithosphärenforschung, Universität Wien, Althanstrasse 14, A-1090 Vienna, Austria;

²⁾ Institut für Mineralogie und Petrographie, Universität Innsbruck, Innrain 52, A-6020 Innsbruck, Austria;

^{†)} Corresponding author, martin.thoeni@univie.ac.at

ABSTRACT

Andalusite-bearing assemblages from a pegmatoid and the Grt-Ky-Bt-flasergneiss host rock from Kienberg, close to the eclogite locality of Gertrusk, Sausalpe, were used to reconstruct a Cretaceous P-T-t path. Garnet core domains from both pegmatoid and gneiss are chemically homogeneous, with high Ca and Mg contents, and rich in rutile inclusions. The inclusion-poor outer parts of the garnet from the gneiss show inhomogeneous element distributions, with increasing Fe and Mn contents towards the rims. Plagioclase and muscovite are inversely zoned, and matrix rutile is rimmed by ilmenite. P-T estimates based on GASP barometry, Zr-in-rutile and Grt-Bt thermometry resulted in peak P-T conditions of c. 1.8 GPa/680-690 °C, and c. 1 GPa/600-640 °C for the time of garnet rim reactions.

Sm-Nd dating of carefully handpicked, H₂SO₄-leached garnet magnetic fractions resulted in a Grt-wr age of 98.6±3.9 Ma for the inclusion-rich garnet cores of the gneiss. The inclusion-poor garnet rim domains yielded 90.8±1.9 Ma for the more Ca-Mg-rich and 86.4±2.9 Ma for the more Fe-Mn-rich fraction. A bulk garnet separate from the pegmatoid yielded an age of 88.0±1.1 Ma. Three biotite fractions from both gneiss and pegmatoid gave concordant Rb-Sr Bt-wr ages of 77.8±1 Ma.

These data and microtextures suggest pegmatoid melt emplacement and andalusite crystallization at Kienberg during decompression/exhumation, documenting the final stages of Cretaceous metamorphism in the eclogite-facies Austroalpine Koralpe-Wölz system, some 90-80 Ma B.P.

Andalusit-führende Paragenesen eines Pegmatoids und von dessen unmittelbarem Nebengestein, eines Grt-Ky-Bt-Flasergneisses von Kienberg (2050 m), 2 km nördlich der bekannten Eklogitlokalität Gertrusk in der zentralen Sausalpe, wurden für die Rekonstruktion eines kretazischen P-T-t-Pfades herangezogen. Die Kernbereiche der Granate sowohl aus dem Pegmatoid als auch aus dem Flasergneis sind chemisch homogen und weisen hohe Ca- und Mg-Gehalte auf; insbesondere jene des Gneises sind reich an Rutileinschlüssen. Die einschlußarmen äußeren Bereiche der Granate des Gneises zeigen eine inhomogene Hauptelementverteilung und steigende Fe- und Mn-Gehalte gegen die Ränder hin. Plagioklas und Muskowit sind invers zoniert, und Matrix-Rutile weisen meist Ilmenitränder auf. Druck-Temperatur-Abschätzungen, basierend auf GASP-Barometrie, Zr-in-Rutil- und Grt-Bt-Thermometrie ergaben ca. 1.8 GPa/680-690 °C für die Bedingungen des Metamorphosepeaks und ca. 1 GPa/600-640 °C für jene der Granatrand-Reaktion.

Sm-Nd-Datierung von optisch ultrarein separierten, magnetisch kontrollierten und H₂SO₄-geleachten Granatfraktionen ergaben ein Granat-Gesamtgesteins-Alter von 98.6±3.9 Ma für die einschlußreichen Granatkernbereiche des Gneises. Die einschlußarmen Granatränder des Gneises gaben ein Alter von 90.8±1.9 Ma für die Ca-Mg-reichen inneren Domänen, während die Fe-Mn-reichen äußeren Domänen ein Alter von 86.4±2.9 Ma lieferten. Eine Gesamtgranatfraktion des Pegmatoids hat ein Grt-wr Sm-Nd-Alter von 88.0±1.1 Ma (2σ). Drei Biotitfraktionen aus Gneis und Pegmatoid zeigen konkordante Rb-Sr-Alter von 77.8±1 Ma.

In Verbindung mit den petrographischen, mikrostrukturellen und mikrochemischen Daten belegen die neuen Altersergebnisse späte Platznahme des Kienberg-Pegmatoids und Kristallisation von Andalusit als Teil einer lokalen Dekompressionsschmelze, die im Zuge der initialen Exhumation in der Endphase des kretazischen tektono-metamorphen Ereignisses, im Zeitraum 90-80 Ma vor heute, in den eo-Alpin eklogitfaziell geprägten Serien des Koralpe-Wölz Systems gebildet wurde.

1. INTRODUCTION

Andalusite is a key mineral for pressure-temperature estimates in metamorphic rocks and typically formed at low-pressure conditions. In addition, andalusite is frequently found in low-P contact metamorphic environments. During high-pressure overprints, andalusite is generally altered, mostly trans-

formed into kyanite and hardly ever metastably preserved.

In the Austroalpine units of the Eastern Alps, regional metamorphic andalusite is known mainly from pre-Alpine (Variscan) rocks, e.g. the Silvretta (Hoernes, 1971) and the northwestern Ötztal-Stubai basement units (Purtscheller, 1969; Tropper and

Hoinkes 1996; Schweigl, 1995), where Alpine tectonothermal overprinting is very weak or absent (Fig. 1). In these areas, andalusite is often associated with late quartz veins and thought to have formed during decompression, post-dating the crystallization of kyanite and sillimanite along a coherent clockwise Variscan P-T loop (Tropper and Hoinkes, 1996).

In this paper, we examine the petrography, mineral chemistry, and age relationships of an andalusite-bearing pegmatoid and its host rock from the central Saualpe (Fig. 1), an area dominated by an eclogite facies-grade Alpine metamorphic overprint and intense deformation in order to (i) characterize in detail the unique andalusite-bearing outcrop at Kienberg and its country rock; (ii) study the potential of conventional bulk multi-grain ID-TIMS geochronometers for precise dating of different steps of a coherent P-T loop, by a combination of optical, magnetic and microchemical criteria of sample preparation and control; (iii) discuss these results within the frame of other Cretaceous high-metamorphic areas of the Austroalpine units.

2. GEOLOGICAL SETTING

The Saualpe is a part of the greater Koralpe-Wölz nappe system (Schmid et al., 2004), large parts of which are characterized by a Cretaceous (eo-Alpine) eclogite facies metamorphism (c. 2-2.5 GPa/700 °C) and intense deformation. However, some parts of this complex nappe pile were subducted to much shallower depths, resulting in significantly lower eo-Alpine peak conditions (c. 1 GPa/600 °C) and hence preserving more extensively the pre-Cretaceous mineralogy and texture (e.g., Thöni and Miller, 2009). In addition, evidence for a pre-Cretaceous metamorphism of Permian age was also de-

tected in many Alpine high-grade assemblages of the Saualpe-Koralpe region (Habler and Thöni, 2001; Habler et al., 2007b). It has been argued that andalusite formed on an orogen scale in the southern Austroalpine units during the Permian low-P extension event (Schuster et al., 2001; Schuster and Stüwe, 2008). Up to now, only textural relics of this mineral have been reported from the Koralpe and Saualpe as up to dm-sized paramorphs that may even preserve the original euhedral andalusite shape (e.g., "Paramorphosenschiefer" in the Koralpe; Beck-Mannagetta, 1980). In these paramorphs, andalusite has completely recrystallized into fine-grained kyanite during the eo-Alpine high-P metamorphic overprint (Habler et al., 2007b). On the other hand, well-preserved Permian andalusite was reported from other Austroalpine domains much further to the west, e.g., from the western Matsch "nappe", an allochthonous unit in the hanging-wall of the southern Ötztal-Stubai Complex (Habler et al., 2007a; Habler et al., 2009).

Recently, metamorphic andalusite of Alpine age has been reported from the SW Schneeberg Complex (Habler et al., 2001) (Fig. 1). Based on petrographic-microstructural and geochronological evidence, this andalusite is interpreted to have formed during decompression/early exhumation of the amphibolite-facies-grade "Schneeberg Normal Fault" rocks, 90-80 Ma ago (Sölva et al., 2005).

Andalusite from the western flank of Kienberg in the Saualpe was first described by Meixner (1953; location no. 4 on his sketch map). In this short report, Meixner (1953) suggests that the andalusite represents the unaltered relictic precursor mineral of the associated Ky-paramorphs.

The locality of Kienberg described in the present study is situated at the top of the north-south trending ridge of the Sau-

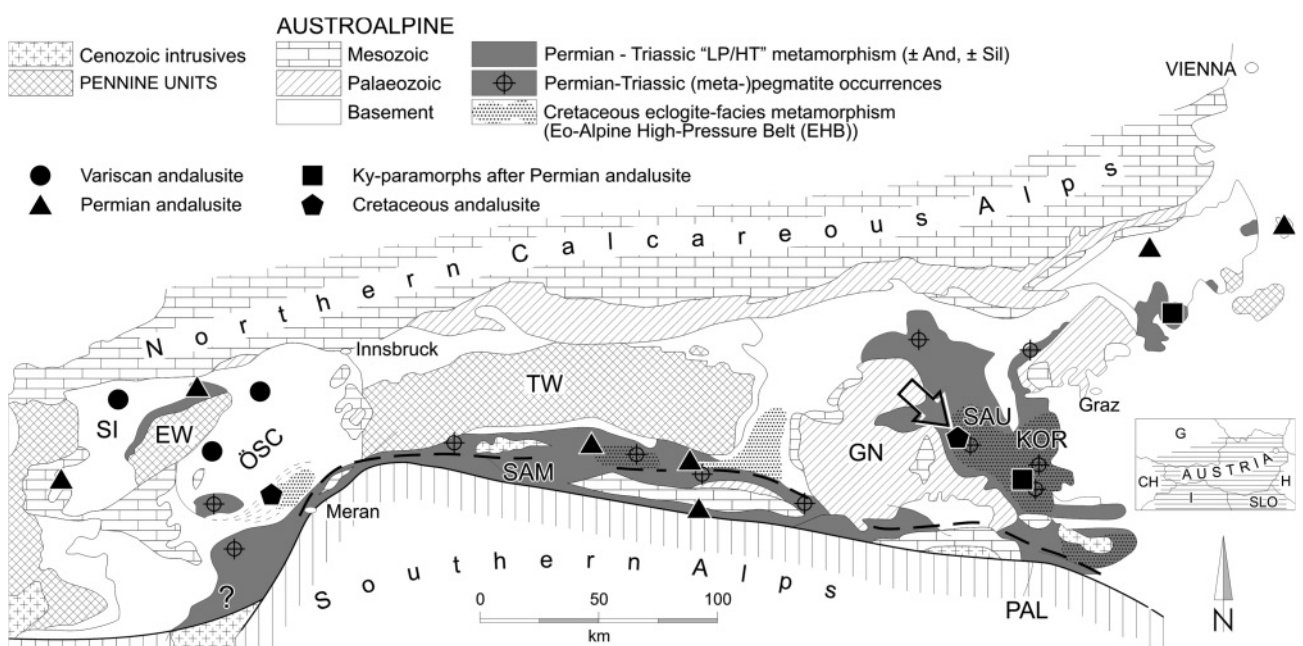


FIGURE 1: Simplified geological-structural map of the Eastern Alps, showing the distribution of metamorphic andalusite of different age within the Austroalpine basement units and the sample locality at Kienberg (large open arrow). SI = Silvretta, ÖSC = Ötztal-Stubai Complex, SAU = Saualpe, KOR = Koralpe, EW = Engadine Window, TW = Tauern Window, GN = Gurktal Nappe system, SAM = Southern limit of strong Alpine (Cretaceous) Metamorphism, PAL = Periadriatic Lineament.

alpe (at 2050 m a.s.l.; Fig. 1), only 2.2 km north of the well-known eclogite outcrop of Gertrusk (2044 m a.s.l.). P-T conditions and age of the Gertrusk eclogite were recently estimated at 2-2.4 GPa / 650-700 °C at 91 ± 1 Ma (Miller et al., 2005; Thöni et al., 2008a).

3. METHODOLOGY

3.1 MICROPROBE, MINERAL CHEMISTRY

Mineral compositions were determined by wavelength-dispersive X-ray analysis using the JEOL JXA-8100 Superprobe at the University of Innsbruck. Analytical conditions were 15 kV accelerating potential and a beam current of 10 nA. Natural and synthetic silicates and oxides were used as standards and a PhiRhoZ routine for matrix corrections. Accessory phases were identified using back-scattered electron (BSE) imaging, energy-dispersive spectroscopy and Raman micro-spectrometry. Trace elements in rutile were analysed with a beam current of 150 nA and counting times of 300 sec for the Zr peak and 150 sec for the Zr background counts. As suggested by Zack et al. (2004), Si concentrations were measured to detect beam overlap with adjacent silicates. Before and after each analytical session, the accuracy of the analyses was checked against rutile standards provided by T. Zack.

Mineral abbreviations are after Siivola and Schmidt (www.bgs.ac.uk/scmr/home.html).



FIGURE 2: Outcrop at Kienberg showing pegmatoid layer oriented sub-parallel to the main foliation of the Grt-bearing Ky-Bt-flasergneiss country rock.

3.2 SM-ND AND RB-SR ISOTOPE ANALYSIS

The Sm-Nd and Rb-Sr analytical work was performed at the Laboratory of Geochronology, Center for Earth Sciences, University of Vienna. Carefully handpicked, either inclusion-rich or optically inclusion-free pure garnet separates used for Sm-Nd analysis weighed between 46 and 77 mg. Before decomposition, or leaching, the fractions were washed for 30 min in warm (70 °C) 2.5 N HCl. Leaching procedures applied followed Anczkiewicz and Thirlwall (2003; using concentrated H_2SO_4). Pure mica concentrates (> 99 %) were obtained by repeated grinding in an agate mill using alcohol, drying and sieving, and finally, magnetic purification. Chemical sample digestion, isotope dilution, and element separation for Sm-Nd and Rb-Sr analysis follow those given in Thöni et al. (2008a). Total procedural blanks were < 1 ng for Rb and Sr, and < 50 pg for Nd and Sm. Sm, Nd, and Sr were run as metals from a Re double filament, using a Finnigan[®] MAT262 (for ID) and a Thermo Finnigan[®] Triton TI TIMS (for IC), while Rb was evaporated using a Ta filament. A $^{143}Nd/^{144}Nd$ ratio of 0.511844 ± 0.000006 (2σ ; $n = 24$) and a $^{87}Sr/^{86}Sr$ ratio of 0.710261 ± 0.000018 (2σ ; $n = 54$) were determined for the La Jolla (Nd) and the NBS987 (Sr) international standards, respectively, during the c. 1 year period of investigation. Within-run mass fractionation for Nd and Sr isotope compositions (IC) was corrected for relative to $^{146}Nd/^{144}Nd = 0.7219$, and $^{86}Sr/^{88}Sr = 0.1194$, respectively. Uncertainties on the $^{143}Nd/^{144}Nd$ and the $^{87}Sr/^{86}Sr$ isotope ratios are quoted as $2\sigma_m$. For the $^{147}Sm/^{144}Nd$ and the $^{87}Rb/^{86}Sr$ ratios, a mean error of ± 1 % is applied (representing maximum errors), including blank contribution, uncertainties on spike composition, and machine drift; regression calculation is based on these uncertainties and the isochron calculations follow Ludwig (2003). Age calculations are based on decay constants of $6.54 \times 10^{-12} a^{-1}$ for ^{147}Sm (Lugmair and Marti, 1978) and $1.42 \times 10^{-11} a^{-1}$ for ^{87}Rb (Steiger and Jäger, 1977), respectively; age errors are given at the 2σ level. For Nd, a continuous depletion of the upper mantle is assumed throughout geological time, and the following Depleted Mantle (DM) model parameters were used: $^{147}Sm/^{144}Nd = 0.222$, $^{143}Nd/^{144}Nd = 0.513114$ (Michard et al., 1985).

4. RESULTS

The investigated outcrop of Kienberg at the top of the Saualpe (2050 m a.s.l.) exposes a pegmatitic layer of about 0.5 m in thickness within a fine-grained Grt-bearing Ky-Bt-paragneiss ("Ky-flasergneiss") (Fig. 2). Six samples from the pegmatoid and eight samples from the country gneiss have been studied in thin section. Samples 07T04SKa (pegmatoid) and 07T04SKb (Grt-bearing Ky-Bt-gneiss) that were used for mineral analysis and geochronological studies are described in detail below.

4.1 PETROGRAPHY AND MINERAL CHEMISTRY

4.1.1 PEGMATOID (07T04SKA)

The pegmatoid is moderately coarse-grained and almost en-

tirely composed of quartz, Na-rich plagioclase and muscovite, with minor garnet, biotite, kyanite, fluorapatite, monazite, zircon, rutile/ilmenite and secondary Fe-Mg-chlorite. Andalusite is present locally, rarely forming euhedral grains, often with granulated rims and/or mantled by polycrystalline muscovite aggregates. In some instances, it shows poikiloblastic growth. Macroscopically, the conspicuously pink, coarse-grained andalusite forms up to 0.5 cm wide “veins” that cut the weak foliation discordantly (Fig. 3). Andalusite grains are optically zoned, with dark pink patches being distinctly more Fe-rich than light-coloured domains (Table 1). Andalusite may contain inclusions of quartz, muscovite, fluorapatite, zircon and rutile partly replaced by ilmenite (Fig. 4a). Garnet is anhedral and frequently forms irregular grain aggregates (Fig. 4b). It is inversely zoned, with rims being distinctly enriched in Alm and Sps ($\text{Alm}_{74-75}\text{Prp}_{10-13}\text{Grs}_{8-10}\text{Sps}_{4.4-6.7}$) compared to interior domains ($\text{Alm}_{59-61}\text{Prp}_{23-24}\text{Grs}_{14-16}\text{Sps}_{1.0-1.3}$). This compares well with compositions determined on hand-picked garnet grains that range from $\text{Alm}_{61.1}\text{Prp}_{22.9}\text{Grs}_{14.9}\text{Sps}_{1.1}$ to $\text{Alm}_{74.6}\text{Prp}_{10.2}\text{Grs}_{9.9}\text{Sps}_{5.1}$ (Table 1). Garnet may contain inclusions of quartz, rutile, muscovite, biotite, zircon and Zn-Fe-sulfide. Garnet compositions are similar to garnet in the enclosing country rock, but clearly different from spessartine-almandine-rich garnets in felsic magmatic rocks (e.g., Miller and Stoddard, 1981; Thöni et al., 2008b). Plagioclase is inversely zoned with core compositions of Ab_{98-99} and rims of Ab_{85-80} . Muscovite has 3.07-3.12 Si pfu and Na/(Na+K) ratios of 0.10-0.14. Fluorapatite contains 0.2-0.3 wt% MnO and significant amounts of Ce (430-680 ppm) and Nd

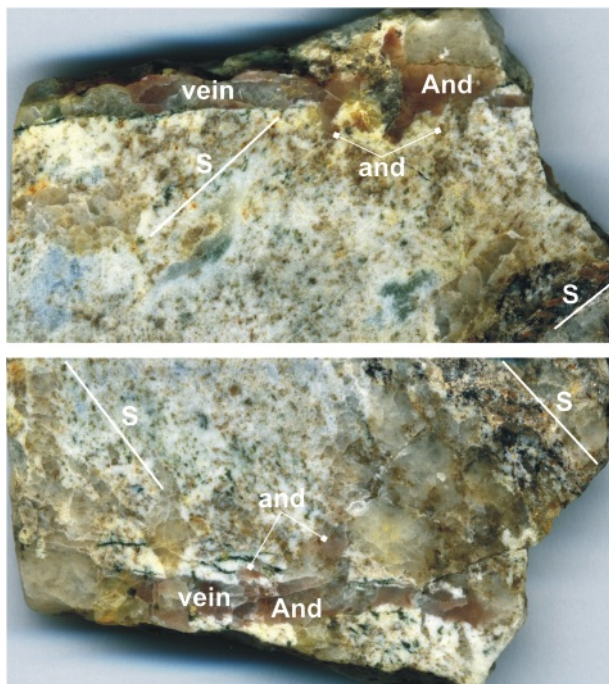


FIGURE 3: Polished specimen of investigated pegmatoid 07T04SKa showing weak orientation of minerals along a tectonic foliation (s) which is crosscut discordantly by a late “vein” filled mainly with quartz and pink andalusite (And). Note that finer grained poikiloblastic/idioblastic andalusite locally also grows within the main fabric (and). Length of specimen is 55 mm.

(600-690 ppm). Cl and F contents range from 0.64-0.82 wt% and from 2.7-3.4 wt%, respectively, implying calculated H_2O contents of less than 0.3 wt% (Table 1). Analysed rutile inclusions in garnet and unreacted rutile in the matrix contain 0.20-0.51 wt% FeO, 382-640 ppm Cr, 3745-4988 ppm Nb and 268-294 ppm Zr (Table 2). Ilmenite frequently replaces rutile. It contains 2.3-2.5 wt% V_2O_5 in addition to 4.0-5.1 wt% MnO and ≤ 1.8 wt% ZnO.

4.1.2 COUNTRY ROCK (GRT-KY-BT FLASER-GNEISS 07T04SKb)

Sample SK07T04b is fine-grained (< 0.5 mm) with a granoblastic texture and consists of quartz, plagioclase, kyanite, garnet, biotite, muscovite, with rutile, ilmenite, zircon, apatite, monazite, tourmaline, graphite and pyrite as accessory phases. Garnet is not abundant, often cracked and partially resorbed, resulting in highly irregular grain shapes (Fig. 5). It may enclose quartz, biotite, muscovite, graphite, rutile, zircon, pyrite and Zn-Fe-sulfide. Kyanite generally forms elongate aggregates, and inclusions in biotite and muscovite. Biotite is partly replaced by Fe-Mg-chlorite, rutile in the matrix is mantled by ilmenite.

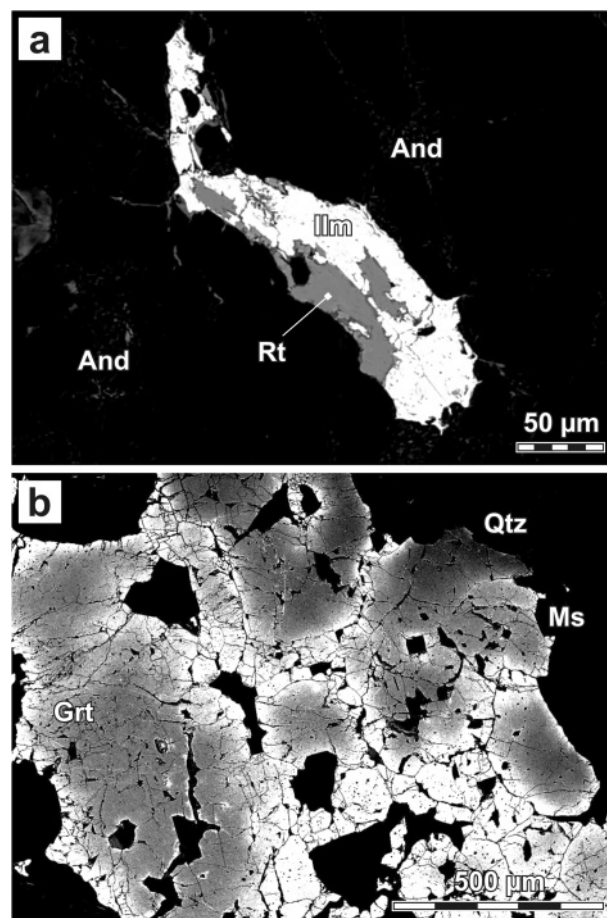


FIGURE 4: (a) BSE image of rutile inclusion in andalusite that has been partly replaced by ilmenite. (b) High-contrast backscattered electron (BSE) image of anhedral garnet from Kienberg pegmatoid 07T04SKa. Note that light-coloured Fe-Mn-rich domains are associated with grain margins, microcracks and mineral inclusions.

Garnet shows compositional zoning. Core compositions are fairly constant ($\text{Alm}_{59-63}\text{Prp}_{21-23}\text{Grs}_{13-16}\text{Sps}_{0.5-1}$), but rim compositions and domains lining biotite±chlorite filled cracks are highly variable, even within the same grain, with $\text{Alm}_{72-75}\text{Prp}_{10-14}$ in addition to spessartine and grossular contents between 2 and

6 mol%, and between 6 and 10 mol%, respectively (Table 1). Analyses of handpicked grains are within the compositional range determined in thin-section. Decreasing Mg/(Mg+Fe) and increasing Mn from core to rim suggest retrograde diffusional zoning, in which pre-existing garnet is modified by

sample 07T04SKa

spot	pink And	pale And	2.4 core Grt	2.4b rim Grt	4.2 core Grt	4.2b rim Grt	10 core PI	11 Ms	4 Ap
SiO ₂	37.08	36.87	38.08	37.15	38.27	37.45	64.92	45.86	0.00
TiO ₂	0.04	0.01	0.02	0.05	0.00	0.02	0.00	0.55	0.00
Al ₂ O ₃	61.94	62.53	21.61	21.13	21.70	21.18	21.87	36.07	0.00
Cr ₂ O ₃	0.01	0.00	0.00	0.00	0.00	0.00	0.00	0.00	0.00
FeO _{TOT}	0.78	0.26	29.36	33.31	28.45	31.45	0.00	0.83	0.11
MnO	0.02	0.00	0.70	2.23	0.64	1.66	0.00	0.00	0.21
MgO	0.12	0.00	5.70	2.55	5.34	2.98	0.00	0.53	0.00
CaO	0.00	0.00	4.28	3.44	5.57	4.89	2.86	0.00	54.71
Na ₂ O	0.00	0.00	0.00	0.00	0.00	0.00	10.03	0.98	0.01
K ₂ O	0.00	0.00	0.00	0.00	0.00	0.00	0.10	10.10	0.00
P ₂ O ₅	n.a.	n.a.	n.a.	n.a.	n.a.	n.a.	n.a.	n.a.	41.76
Cl	n.a.	n.a.	n.a.	n.a.	n.a.	n.a.	n.a.	n.a.	0.64
F	n.a.	n.a.	n.a.	n.a.	n.a.	n.a.	n.a.	n.a.	3.41
Total	99.99	99.67	99.75	99.86	99.97	99.63	99.78	94.92	100.85

sample 07T04SKb

spot	1.10 core Grt	1.9 rim Grt	10 rim Grt	1,12 Bt	18 Bt	21 Ms	2 core PI	1.8 rim PI	5 Ky	Chl
SiO ₂	38.32	37.51	37.37	34.47	36.39	46.68	65.31	63.55	37.02	24.51
TiO ₂	0.02	0.02	0.03	1.18	1.33	1.14	0.04	0.00	0.01	0.02
Al ₂ O ₃	21.79	21.15	21.20	19.51	19.19	32.49	21.35	22.51	62.27	23.37
Cr ₂ O ₃	0.00	0.00	0.00	0.00	0.00	0.00	0.00	0.00	0.00	0.00
FeO _{TOT}	28.26	32.41	32.53	21.34	20.53	1.25	0.30	0.28	0.38	26.83
MnO	0.73	1.89	2.10	0.03	0.14	0.02	0.00	0.00	0.01	0.22
MgO	5.82	3.44	3.20	8.42	8.73	1.18	0.00	0.02	0.00	13.96
CaO	5.15	3.49	3.39	0.00	0.00	0.00	2.29	3.96	0.00	0.00
Na ₂ O	0.00	0.00	0.00	0.12	0.12	0.80	10.32	9.39	0.00	0.00
K ₂ O	0.00	0.00	0.00	9.77	9.45	10.76	0.08	0.11	0.00	0.00
P ₂ O ₅	n.a.	n.a.	n.a.	n.a.	n.a.	n.a.	n.a.	n.a.	n.a.	n.a.
Cl	n.a.	n.a.	n.a.	n.a.	n.a.	n.a.	n.a.	n.a.	n.a.	n.a.
F	n.a.	n.a.	n.a.	n.a.	n.a.	n.a.	n.a.	n.a.	n.a.	n.a.
Total	100.09	99.91	99.82	94.84	95.88	94.32	99.69	99.82	99.69	88.91

n.a. = not analysed

TABLE 1: Representative electron microprobe analyses of minerals from Kienberg pegmatoid (07T04Ka) and country rock (07T04SKb).

exchange of material with the rock matrix.

Plagioclase is inversely zoned with core compositions of Ab_{94-90} and rims of Ab_{86-80} . Analysed biotite has $Mg/(Mg+Fe)$ values between 0.40 and 0.44, and Ti and Al^M contents in the range of 0.05-0.13 and 0.40-0.51, on the basis of 11 oxygens. Muscovite is zoned, with core compositions (3.2-3.3 Si pfu) being more phengitic than rims (3.0-3.1 pfu). Individual rutile grains included in garnet and in the matrix are homogeneous, and contain 0.18-0.58 wt% FeO, 382-1091 ppm Cr, 1211-4216 ppm Nb and 260-308 ppm Zr (Table 2). Low Cr (< 1000 ppm) and high Nb contents (> 900 ppm) are typical of rutile in meta-pelitic rocks (Zack et al., 2004b). In the matrix, ilmenite replaces rutile. It is Mn- and Zn-rich, containing 2.1-2.4 wt% MnO and 3.0-3.1 wt% ZnO in addition to 2.5-2.9 wt% V_2O_5 .

4.2 RADIOGENIC ISOTOPES AND GEOCHRONOLOGY

4.2.1 SM-ND DATA

Nine Sm-Nd analyses, including two whole rock powders and results from different garnet separates, carefully handpicked from defined sieve and magnetic fractions (= MF, either untreated or leached with conc. H_2SO_4) are listed on Table 3a and

plotted in isochron diagrams (Fig. 6a-d). One garnet separate of the pegmatoid (sample 07T04SKa) and four different garnet fractions were analyzed from the Grt-Ky-Bt gneiss enclosing the pegmatoid (= country rock; sample 07T04SKb), three of which were treated with the H_2SO_4 leaching technique (Anczkiewicz and Thirlwall, 2003) before dissolution to eliminate any un-equilibrated REE-rich inclusions and to maximize the spread in Sm/Nd. The need for application of this technique was a consequence of the first pilot analysis of the unleached, low-spread garnet separate (Table 3), handpicked from the bulk crushate of the 0.16-0.45 mm sieve fraction. Abbreviations used in Table 3 and Fig. 6: R = residual garnet fraction, L = leachate (Nd-rich inclusions).

a) Inclusion-rich, Fe-Mn-poor garnet core domains from Grt-Ky-Bt gneiss (= Grt GI R; Fig. 6a)

The bulk crushate of the pegmatoid host gneiss contained a considerable amount of darkly pigmented, inclusion-rich fragments of garnet. Microtextural observations and microchemical data suggested that these pigmented domains represent garnet cores (Fig. 5b) and, thus, perhaps were relics retaining a Nd isotopic memory of an older (pre-Cretaceous) garnet generation. Microprobe analysis of garnet in thin section and of garnet grain fragments from the fraction that was used

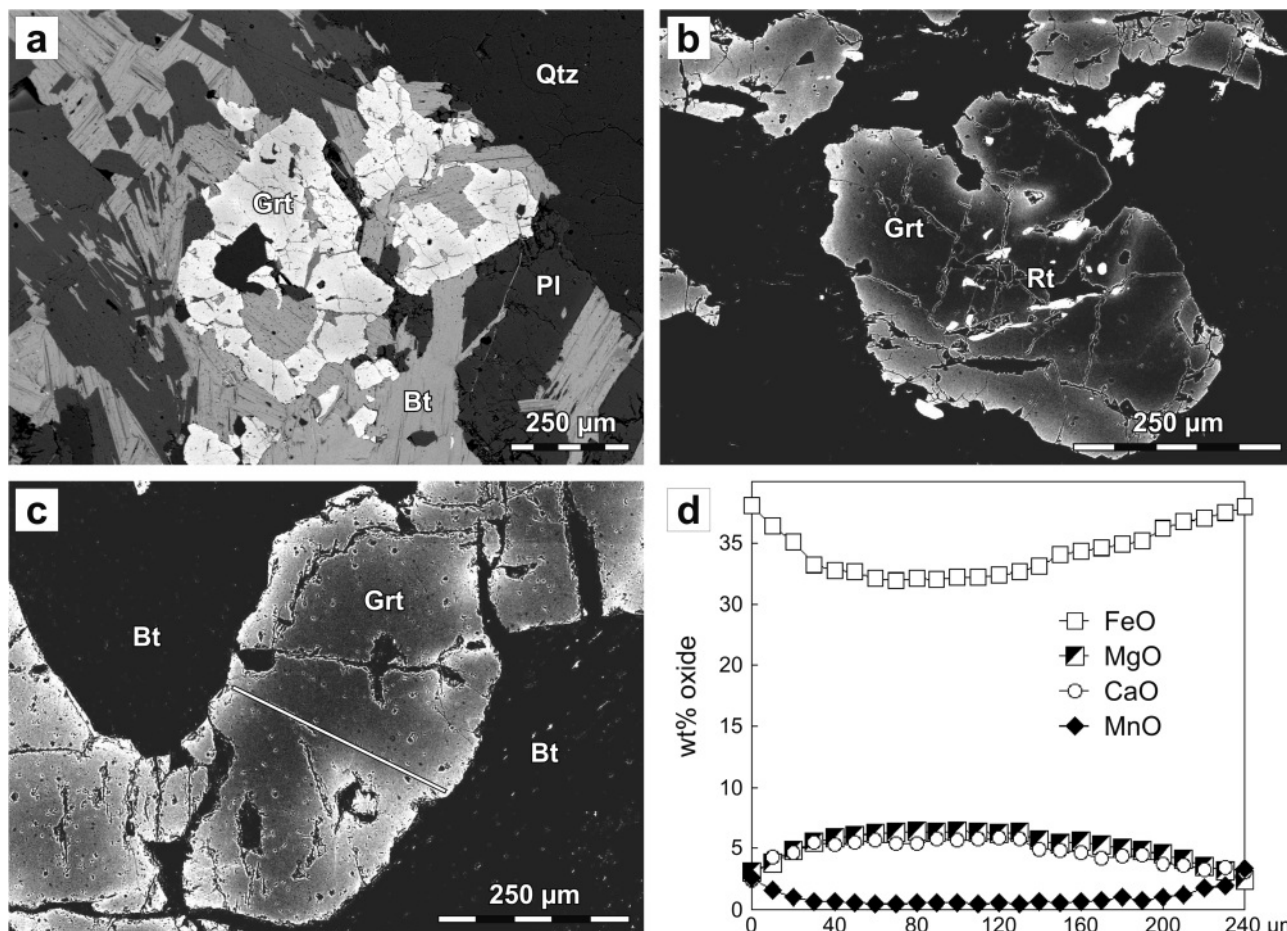


FIGURE 5: BSE images (a-c) illustrating micro-textures of anhedral garnet in pegmatoid host rock 07T04SKb. The light-coloured domains along margins and microcracks seen in the high-contrast BSE images (b) and (c) are Fe-Mn-rich. Note rutile inclusions in the core domain of garnet (b). (d) Chemical zoning profile of garnet along line shown in (c).

for Sm-Nd isotope analysis showed that these domains are fairly homogeneous, with high pyrope- and grossular-contents if compared with the inclusion-poor outer domains. A hand-picked grain separate from this strongly pigmented species was leached with hot concentrated H₂SO₄. Although the leached residual garnet fraction R showed a rather moderate spread in Sm/Nd (¹⁴⁷Sm/¹⁴⁴Nd = 0.365, Table 3a), both regression with the analysed leachate (= dissolved inclusions), and with the whole rock, clearly indicate an eo-Alpine garnet growth, with ages of 98.6±3.9 Ma (Grt core R–wr), 99.4±4.1 Ma (Grt core R–L), and 98.9±3.7 Ma (εNdt = -9.3; MSWD = 0.26), if all data points (n = 3) are included in the regression (Fig. 6a). This result also indicates that REE-rich inclusions

This result is, therefore, not used for further geochronological considerations (data point label set in parenthesis on Fig. 6b). b2) H₂SO₄-leached fraction (R). Hot H₂SO₄-leaching of a second garnet bulk separate handpicked from the same sieve fraction resulted in a composition typical for the Sm-Nd systematics of “pure” garnet (0.62 ppm Nd, ¹⁴⁷Sm/¹⁴⁴Nd = 1.17). The well-defined Grt–wr age of 90.8±1.9 Ma (Table 3; Fig. 6b) is identical with the Sm-Nd age measured for high-P metamorphic garnet–omphacite mineral pairs of the nearby Gertusk eclogite (90.6±1.0 Ma; Thöni et al., 2008a). It is also similar to Grt–wr/Grt–mineral ages obtained for pyrope-rich high-P garnet from metapelites (“Schiefergneise”) encasing the mafic eclogites in the high-grade metamorphic central Saualpe (Thöni and Miller, 1996).

sample		No. of spots	Zr ppm	SD	T1°C	T2°C	T3°C
07T04SKa_pegmatoid	Grt-incl	8	274	8	707	635	682
07T04SKa_pegmatoid	Grt-incl	3	286	10	713	639	686
07T04SKa_pegmatoid	matrix	6	272	9	706	635	682
07T04SKb_country rock	matrix	5	260	6	701	631	678
07T04SKb_country rock	matrix	7	306	12	721	644	691
07T04SKb_country rock	Grt-incl	8	272	8	706	635	682
09T03KS_country rock	matrix	7	290	9	715	640	687
09T03KS_country rock	Grt-incl	7	276	10	708	636	683
09T03KS_country rock	matrix	8	269	8	705	634	681
09T03KS_country rock	matrix	4	308	11	722	645	692
09T03KS_country rock	Grt-incl	3	273	14	707	635	682

T1 = Zack et al. (2004), T2 = Watson et al. (2006); T3 (at 1.8 G Pa) = Tomkins et al. (2007)

TABLE 2: Zr in rutile analyses for Kienberg samples.

and garnet host were in Nd isotopic equilibrium at the time of early (“core”) garnet crystallization (i.e., they are more or less cogenetic) and that no pre-Cretaceous garnet relics can be detected in this assemblage using the Sm-Nd geochronometric/geochemical tracer system. In addition, the result is within the limits of analytical errors still overlapping with the high-P garnet core-age of 94.1±0.8 Ma from the nearby Gertusk eclogite (Thöni et al., 2008a).

b) Inclusion-poor, Fe-Mn-poor garnet separate from Grt-Ky-Bt gneiss (= Grt GIIa 2MF; Fig. 6b)

b1) unleached fraction. Analysis of a separate handpicked from this fraction resulted in a very low ¹⁴⁷Sm/¹⁴⁴Nd ratio (0.226) and a high Nd concentration of 7.2 ppm that suggested presence of a considerable amount of LREE-rich micro-inclusions (Table 3a). However, as shown by the leaching experiment of the same garnet (Fig. 6b) and in contrast to Grt cores (Grt GI, above), the inclusions are not in Nd isotope equilibrium with the host mineral. The spurious, moderately precise (low-spread) Grt–wr “age” result was 66.6±6.7 Ma.

c) Bulk garnet separate from the pegmatoid, sample 07T04SKa (= GrtP; Fig. 6c)

The garnet GrtP, handpicked from the pegmatoid bulk crushate, was treated as a single fraction; because of its optically fairly inclusion-free nature, no leaching was applied to this material. GrtP–wr regression resulted in an age of 88.0±1.1 Ma, with εNd(t) = -9.4 (Fig. 6c).

d) Fe-Mn-rich magnetic fraction, Grt “rims” (1 MF) from Grt-Ky-Bt gneiss (Grt GIIb R; Fig. 6d),

A Fe-Mn-rich separate was also handpicked from the garnet bulk crushate of the gneiss, using the strongest magnetic (1MF) garnet fraction. This separate yielded a nominally somewhat younger Grt–wr age result of 86.4±2.9 Ma, although within analytical errors still overlapping

with the age obtained from Grt GIIa (2MF). As expected, the data point for the leachate (L) typically lies off the Grt R–wr tie line, indicating that the leached inclusions are, again, not in Nd isotope equilibrium with the garnet host (Fig. 6d). The 86 Ma age ranges among the youngest garnet ages measured so far from the Cretaceous metamorphic areas of the Austroalpine units (e.g., Thöni, 2002). It may be interpreted as the time of garnet rim growth, or the end of Nd isotope exchange between garnet rims and matrix minerals, in the course of eo-Alpine decompression and cooling.

e) Nd isotopes in the bulk rocks

Comparison of the whole rock Nd isotopic composition of the pegmatoid and the host Grt-Ky-Bt-gneiss shows them to be almost identical, with a typical crustal composition and present-day εNd values at -10.3 (pegmatoid) and -10.1 (gneiss) that strongly support a genetic relationship of their sources (Table 3a). Depleted mantle model ages are 1.39 Ga for the pegmatoid and 1.63 Ga for the gneiss. This implies that the “pegmatite” does not represent an igneous product derived

from an unknown magmatic source, but rather a local segregation produced \pm *in situ* during marked pressure drop and fluid release (“pegmatoid”).

4.2.2 Rb-Sr DATA

The Rb-Sr analytical data for one biotite fraction, one white mica fraction, and the whole rock from the pegmatoid (07T04SKa) and for two magnetically slightly different biotite fractions and the whole rock of the host Grt-Ky-Bt gneiss (07T04SKb) are listed in Table 3b. All biotites yield perfectly concordant mineral–wr ages at 77.8 ± 1 Ma, in line with the regional mica age trend. The white mica–wr age result for the pegmatoid plots off this trend; this “age”, however, is not considered very

coarse-grained white mica is known to behave fairly resistant against complete isotopic resetting during short-lived thermal and deformational overprints (e.g., Morauf, 1981).

5. DISCUSSION

5.1 THERMOBAROMETRY

Garnet from both pegmatoid and country rock is characterized by homogeneous pyrope-grossular-rich and Mn-poor core domains. The absence of any prograde growth zoning commonly observed in garnet from low and medium grade regionally metamorphosed rocks (e.g. Tracy et al., 1976) suggests homogenisation through volume diffusion at tempera-

a)	Sm, ppm	Nd, ppm	$^{147}\text{Sm}/^{144}\text{Nd}$	$^{143}\text{Nd}/^{144}\text{Nd}$	$\pm 2\sigma_m$	Grt–wr age	ϵ (t) Nd
<i>a) Andalusite-bearing pegmatoid</i>							
07T04SKa wr	6.34	34.3	0.1116	0.512108	0.000002		
Grt 0.16-0.45 bulk	3.51	1.37	1.5493	0.512935	0.000006	88.0 \pm 1.1	-9.4
<i>b) Grt-Ky-Bt gneiss (host rock)</i>							
07T04SKb wr	3.49	16.3	0.1292	0.512119	0.000003		
Grt GI (cores), R (H ₂ SO ₄)	1.24	2.05	0.3652	0.512271	0.000004	98.6 \pm 3.9	-9.2
" , L (H ₂ SO ₄)	5.25	20.1	0.1580	0.512136	0.000002		
Grt GIIa 0.16-0.45 2MF, h.p. (n.l.)	2.70	7.22	0.2258	0.512161	0.000002		
Grt GIIa 0.16-0.45 2MF, R (H ₂ SO ₄)	1.20	0.618	1.1726	0.512738	0.000011	90.8 \pm 1.9	-9.3
Grt GIIb 0.16-0.45 1MF, R (H ₂ SO ₄)	1.28	1.12	0.6866	0.512434	0.000009	86.4 \pm 2.9	-9.4
" , L (H ₂ SO ₄)	4.06	15.7	0.1567	0.512158	0.000003		
b)	Rb, ppm	Sr, ppm	$^{87}\text{Rb}/^{86}\text{Sr}$	$^{87}\text{Sr}/^{86}\text{Sr}$	$\pm 2\sigma_m$	wr–mineral age	
<i>a) pegmatoid</i>							
07T04SKa wr	61.8	275	0.6515	0.723719	0.000004		
Ms 0.16-0.45	311	161	5.6059	0.731626	0.000004	(112.3 \pm 1.3)	
Bt 0.16-0.45	437	8.95	143.77	0.882003	0.001789	77.8 \pm 1.2	
<i>b) Grt-Ky-Bt gneiss (host rock)</i>							
07T04SKb wr	136	171	2.3090	0.725700	0.000005		
Bt 0.16-0.45, 1MF	530	3.58	449.79	1.220903	0.000053	77.9 \pm 0.8	
Bt 0.16-0.45, 2MF	541	4.08	401.08	1.166399	0.000018	77.8 \pm 0.8	

TABLE 3: a) Sm-Nd data for garnet fractions and whole rocks of And-bearing pegmatoid and Grt-Ky-Bt-flasergneiss (Kienberg). b) Rb-Sr data for mica fractions and whole rocks of Kienberg And-bearing pegmatoid and Ky-Grt-Bt-flasergneiss (Sausalpe).

robust, due to the rather low Rb/Sr ratio of this Sr-rich white mica, and perfect equilibration of Sr isotopes at the time of closure of the white mica may not have been effective in the system. Alternatively, this “age” could also be interpreted to retain some pre-peak (subduction-related), or even presubduction isotopic memory (provided that the pegmatoid crystallized from a pre-existing metamorphic assemblage), since

tures in excess of 615–665 °C (e.g. Yardley, 1977). On the other hand, the presence of stable muscovite indicates that PT conditions reached in the Ky zone did not induce pervasive melting.

In order to obtain better constraints on peak metamorphic temperatures, rutile grains in three samples were analysed for Zr as recent studies demonstrated a temperature depen-

dence of Zr in rutile in quartz + zircon-bearing rocks (Zack et al., 2004a; Watson et al., 2006; Ferry and Watson, 2007). In order to assess homogeneity, three to eight spot analyses were collected on each grain. The results show that rutile is unzoned and that compositions of rutile grains included in Mn-poor garnet domains are similar to those of unreacted matrix rutile. Zr variations are quite limited, suggesting an approach to Zr equilibrium distribution between rutile and zircon at temperatures between 701-722 °C using the empirical calibration of Zack et al. (2004a). The calibration of Watson et al. (2006) that is based on experimental data performed mainly at 1 GPa yielded lower temperatures ranging from 631 to 645 °C (Table 2). This discrepancy, however, can be resolved when taking

into account the pressure dependence of the Zr-in-rutile thermometer (Degeling, 2003; Troitsch and Ellis, 2004). Pressures were calculated with the GASP barometer, using the calibration of Koziol and Newton (1988). For garnet in samples 07T04SKa and 07T04SKb, the maximum grossular value of 16 mol% yields pressures of about 1.8 GPa using plagioclase core compositions and assuming temperatures of 680-700 °C. The new pressure-corrected Zr-in-rutile thermometer calibration of Tomkins et al. (2007) results in temperatures ranging from 671-692 °C at 1.8 GPa (Table 2).

In contrast, Mn-rich garnet domains that contain distinctly less pyrope and grossular components compared to cores are associated with grain margins, biotite-filled micro-cracks

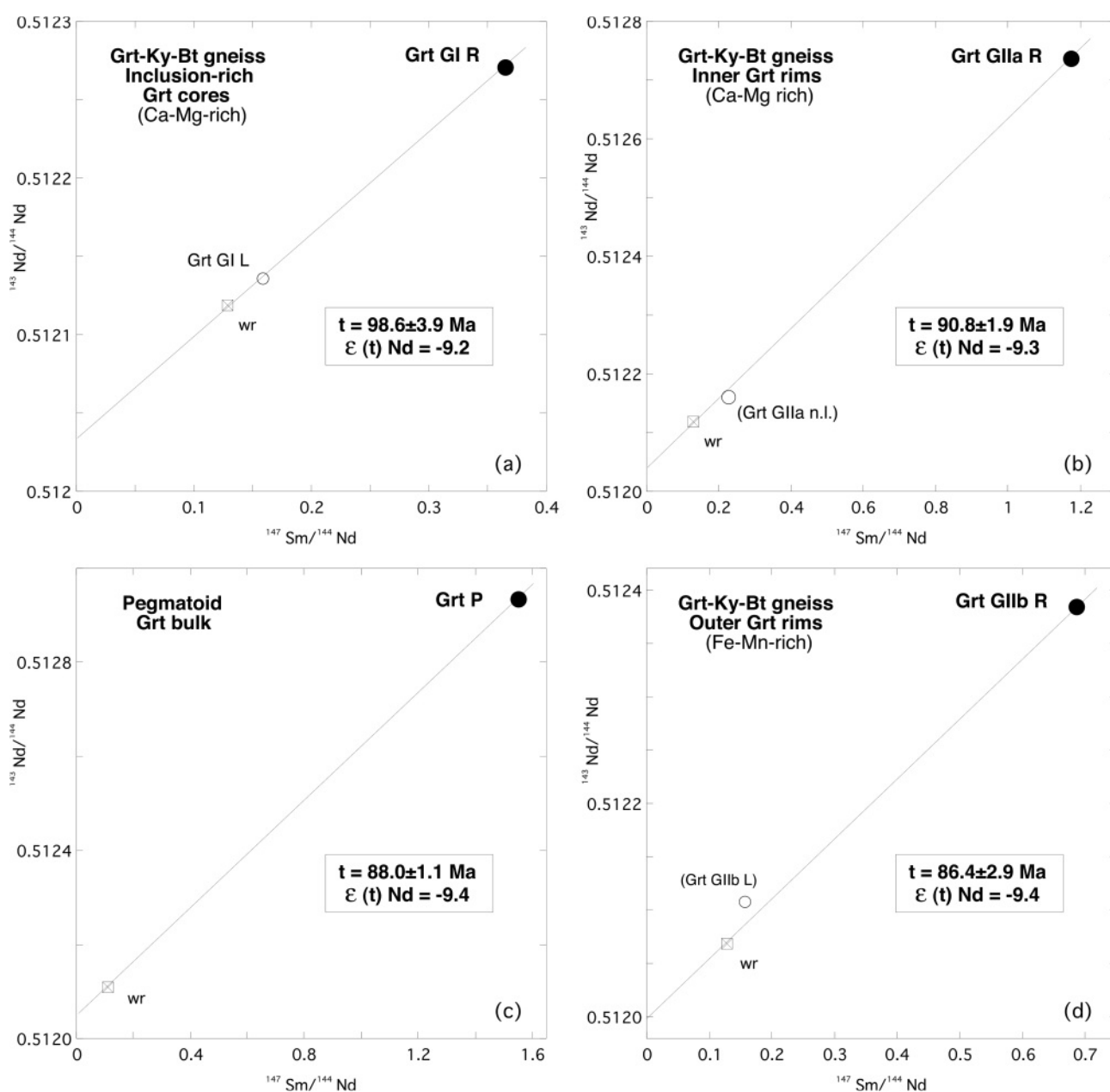


FIGURE 6: Sm-Nd isochron diagrams for whole rocks and garnet fractions of Grt-Ky-bearing Bt-Pl-flasergneiss 07T04SKb (a, b, d) and andalusite-bearing pegmatoid layer 07T04SKa (c). The different Grt-wr ages in (a)-(d) are interpreted to reflect subsequent evolution steps during a single coherent P-T loop in the Cretaceous (see text for explanation, and Fig. 7). Data point labels set in parenthesis are not considered for age calculation. Note that symbol size exceeds bars for analytical errors in all cases.

and biotite inclusions (Fig. 4, 5). Since garnet coexists with kyanite and inversely zoned plagioclase, decreasing grossular could be explained by the reaction $\text{Grs} + 2 \text{Ky} + \text{Qtz} = \text{An}$ (GASP). The pattern of decreasing grossular in the garnet grains is consistent with growth under conditions of decreasing pressure because grossular is on the high-P side of the GASP reaction. For a grossular component of 9 mol% in garnet domains touching biotite and plagioclase rims, pressures of 0.9–1.0 GPa are obtained for a temperature range of 600–640 °C that is based on the garnet-biotite geothermometer of Kleemann and Reinhardt (1994). This indicates that the rocks have undergone a significant pressure drop and cooling during their early retrograde evolution. The appearance of stable andalusite suggests additional isothermal decompression to $P < 0.4$ GPa.

5.2 CORRELATION OF (MICRO-)STRUCTURAL OBSERVATIONS, P-T DATA AND GEOCHRONOLOGY – THE AGE OF ANDALUSITE AND EMPLACEMENT OF THE PEGMATOID

The fact that cm-sized andalusite-rich “veins” crosscut the observed weak schistosity of the pegmatoid that is partly defined by fine-grained kyanite indicates a late crystallization of andalusite, post-dating the major deformation in the rocks (Fig. 3). In addition, the observation that andalusite may contain rutile inclusions which are partly replaced by ilmenite (Fig. 4a) argues for a post-high-P crystallization of this mineral.

Meixner (1953) suggested that the andalusite from the west flank of Kienberg escaped transformation into kyanite within the Ky-flasergneiss, the Saualpe analogue of the Koralpe “Paramorphosenschiefer” series. Since the precursor andalusite in the “Paramorphosenschiefer” of the Koralpe that crystallized in the course of the long-lived Permian-Triassic low-P metamorphic event (Habler and Thöni, 2001; Habler et al., 2007b) is completely replaced by kyanite, Meixner’s (1953) assumption would imply that the Kienberg andalusite records a pre-kyanite (= pre-Cretaceous) metamorphic history. Though Meixner (1953, 1975) refers to a somewhat different outcrop level of Kienberg (at 1800 m a.s.l.; see Mörtl, on-line publ.), it is highly improbable that unaltered euhedral pre-Cretaceous andalusite could escape transformation into kyanite during the Cretaceous subduction and high P-T metamorphic overprint.

As the “pegmatite” at Kienberg top is aligned roughly parallel to the main foliation of the Grt-Ky-Bt country rock (Fig. 2), its emplacement age relative to the observed macro-mesoscopic structures remains unknown. The whole rock isotope analysis of pegmatoid 07T04SKa gives no information on the time of emplacement, hence the assumption that this “pegmatite” formed in the late Cretaceous, e.g., by decompression during fast exhumation, is not supported by independent field evidence. However, textural/microstructural, mineral chemical-petrological and geochronological data clearly argue for a late Cretaceous formation of this pegmatoid layer, as shown on Fig. 2.

Both composition (Table 1) and Sm-Nd age of the garnet from the pegmatoid (Table 3; Fig. 6c) clearly support this con-

clusion. An integral and characteristic element of the Cretaceous eclogite-facies metamorphic Saualpe-Koralpe crystalline are dm- to > 100-m-sized (meta-)pegmatite layers interpreted to have been formed in the course of the Permian–Triassic extensional event (Morauf, 1981; Heede, 1997; Thöni and Miller, 2000; Habler et al., 2007b; Thöni et al., 2008b; Schuster and Stüwe, 2008, for a review). In addition to coarse-grained muscovite books (Morauf, 1981), zircon (Heede, 1997) and cm-sized spodumene (Thöni and Miller, 2000), garnet is the most conspicuous refractory phase that survived the strong eo-Alpine tectonometamorphic overprint in these rocks, yielding Permian-Triassic Sm-Nd ages. Sm-Nd dating of primary magmatic, generally spessartine-almandine-rich garnet has, therefore, been used as a key tool to constrain the exact age of emplacement of these pegmatites (Habler and Thöni, 2001; Habler et al., 2007b; Thöni et al., 2008b). Correlation of primary, magmatic major element and trace element (REE) zoning and Sm-Nd age is generally clear-cut, while evidence for a metamorphic overprint of garnet is surprisingly minor or absent. In contrast, garnet from the pegmatoid at Kienberg has a distinct major element composition which resembles that of the host gneiss (Table 1); it does not show any evidence of pre-Cretaceous relic domains, neither chemically nor isotopically, and the Sm-Nd age (88 ± 1 Ma) itself proves crystallization essentially after the eo-Alpine pressure peak (estimated at c. 95–90 Ma; Thöni et al., 2008a). At Kienberg the data from both the andalusite-bearing pegmatoid layer and its country

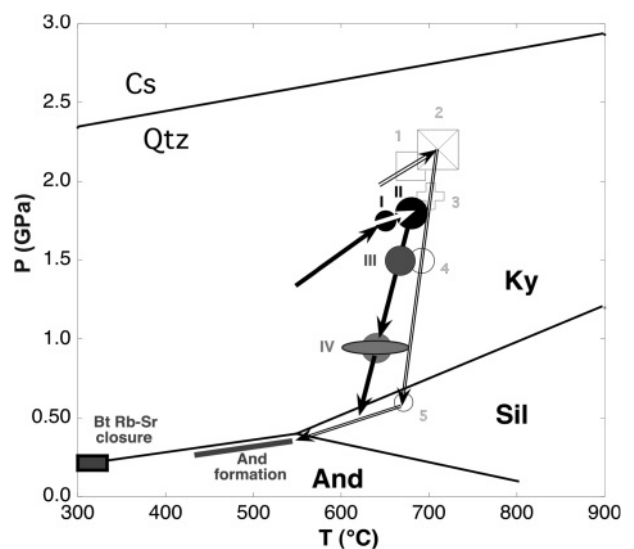


FIGURE 7: P-T-t diagram of the Cretaceous eclogite-facies central Saualpe area, comparing results obtained on the mafic eclogites (open symbols labelled with Arabic numerals are from Thöni et al., 2008a) with P-T-t data from the Kienberg pegmatoid and Grt-Ky-Bt host flaser-gneiss (filled symbols labelled with Roman numerals are data from this study). (I) Ca-Mg-rich garnet cores, rich in rutile inclusions: 98.6 ± 3.9 Ma; (II) final peak P-T conditions in the gneiss: 90.8 ± 1.9 Ma; (III) garnet crystallization in pegmatoid due to local melting during early decompression: 88.0 ± 1.1 Ma; (IV) final garnet rim reaction in gneiss during fast decompression and cooling: 86.4 ± 2.9 Ma. The P-T window for andalusite crystallisation is set at < 0.4 GPa / < 550 - > 450 °C (between c. 86 and 80 Ma), closure of the Rb-Sr system in biotite near 300 °C, at 78 ± 1 Ma.

rock indicate a continuous transition from the high-P kyanite into the andalusite stability field during a single crystallization event, reflecting a pressure/temperature drop from c. 1.8 GPa/700 °C at the metamorphic peak to < 0.4 GPa/< 500 and, finally, < 300 °C (garnet rims, andalusite crystallization, and blocking of Sr diffusion in biotite, respectively) between c. 91±2 and 78±1 Ma (Figs. 6, 7, Table 3). In addition, the host gneiss is characterized by isolated small-scale quartz-feldspar-rich pegmatoid patches, lenses and veins. This suggests that at the final stages of Cretaceous metamorphism (i.e., during early decompression) melting may have occurred locally, though not extensively, as indicated by the ubiquitous persistence of stable muscovite.

The new geochronological data presented in Table 3 and Fig. 6 span a time window of some 19 Ma (including the error limits), i.e., between 98.6±3.9 and 86.4±2.9 Ma for REE reaction in garnet. Since garnet is clearly continuously zoned with respect to major elements, grain internal age zonation is very likely as well and indeed documented by the Sm-Nd results. This may also reflect the fact that metamorphic reactions and strain rates are generally rather fast relative to thermal diffusion rates (e. g., Baxter and DePaolo, 2004). Compared to high-spatial resolution *in situ* analytical techniques (SIMS, LA-ICP-MS, SHRIMP), the destructive bulk multigrain “conventional” (ID-TIMS) isotope analytical methods seem to have clear disadvantages in defining exact age brackets for minerals from complex tectonothermal situations. In special cases, e.g., for cm-sized megacrystals, separation of growth domains by drilling/sawing and individual chemical and isotopic analysis of these domains may be possible (e.g., Thöni and Miller, 2009; Pollington and Baxter, 2010), in order to further resolve a metamorphic P-T-t path. For zoned minerals with a “normal” (millimetre to micrometre) grain size, precise ID-TIMS dating of the different “high-T” (> 500 °C) steps of a tectonometamorphic evolution is a challenge. However, careful separation of tightly-defined magnetic (MF) and grain size (sieve) fractions, combined with microchemical (electron microprobe, LA-ICP-MS for REE) control of splits of the handpicked mineral separates used for isotope analysis strongly improves domain identification and may allow reasonable within-grain age resolution for a “bulk mineral separate” (Fig. 6a-d). In these cases, the potential of Sm-Nd garnet geochronology is rather unique in that radiogenic isotope/precise trace element data of this mineral phase can be directly linked with textural/microstructural, microchemical and P-T information extracted from one and the same material and its assemblage.

In detail, the new Sm-Nd data for garnet are interpreted to reflect the following stages of evolution of a single, coherent P-T loop:

- a) The rutile-pigmented garnet “core” domains of the gneiss (Grt GI) crystallized at high P-T conditions. The 98.6±3.9 Ma (Grt core–wr) Sm-Nd age documents a time window close to the pressure peak (deepest subduction), and may even encompass the final steps of the prograde path, at high pressures.
- b) The 90.8±1.9 Ma Grt–wr Sm-Nd age of the Fe-Mn-poor garnet fraction of the gneiss (representing inclusion-poor garnet interior domains; Grt GIIa 2MF) is interpreted as the time, when final peak P-T conditions were effective (≤ 2 GPa/ ≤ 700 °C).
- c) The 88.0±1.1 Ma Sm-Nd garnet–whole rock age (GrtP–wr) from the pegmatoid is interpreted to date garnet crystallization during fast exhumation, i.e., a rapid pressure drop, possibly inducing local decompression melting in the gneiss. However, since this garnet is significantly zoned with respect to major elements, zonation of trace elements (REE) and age variations (Nd isotopes) are feasible. For this reason, the fairly precise age (analytical uncertainty is close to ± 1 Ma) of the chemically somewhat inhomogeneous bulk mineral separate represents a “mean” age and should not be overestimated, since the true time window for garnet crystallization in the pegmatoid could well exceed the time span of c. 2 Ma. Nonetheless, the age result suggests a somewhat younger age for the mineral assemblage of the pegmatoid, compared to the high-P minerals of the gneiss. Since the pegmatoid itself is weakly foliated (Figs. 2, 3), ductile deformation of feldspar must have outlasted the time of 88±1 Ma (= garnet mean age).
- d) The 86.4±2.9 Ma Sm-Nd Grt rim–wr age (Grt GIIb 1MF) reflects closure of the Sm-Nd isotopic system, when garnet crystallization and/or element exchange between garnet and matrix minerals ceased in the pegmatoid host rock during near-isothermal decompression, at medium PT conditions. This time window probably also marks the end of major ductile deformation in the gneiss (plagioclase, alignment of kyanite and mica).
- e) The Bt–wr Rb-Sr ages at 78±1 Ma reflect closure of the Rb-Sr isotopic system, indicating a drop of effective temperatures in the exhuming wedge in the range < 400 - \geq 300 °C. Summing up, these age results suggest that andalusite at Kienberg top probably crystallized in the time window ≤ 86 - > 80 Ma B.P. (Fig. 7).

6. REGIONAL GEOLOGY AND THE P-T-T PATH OF KIENBERG

For the Cretaceous metamorphic central Saualpe area, minerals and isotopic systems from both, metabasic eclogites and high-P metapelites support a common crystallization/decompression history. The pressure peak was presumably attained between c. 95 and 90 Ma, followed by rather fast isothermal decompression from c. 88±2 Ma onwards, and cooling to c. 400 °C between c. 88 and 83 Ma (Miller et al. 2005; Thöni et al. 2008a). Subsequently, the gradient of the cooling path seems to have flattened out, as derived from ^{40}Ar - ^{39}Ar white mica and Rb-Sr biotite closure ages (Manby and Thiedig, 1988; Wiesinger et al., 2006; Morauf 1981; Thöni and Jagoutz, 1992; Heede, 1997).

The new data from Kienberg top, derived from assemblages containing low-pressure andalusite, fit exceptionally well into this P-T-t path (Fig. 7). The analytical results indicate that the

investigated samples shared the Cretaceous subduction and high-P history, leaving little doubt that andalusite at Kienberg top is not a pre-Cretaceous relic, but rather formed at a late stage of Cretaceous exhumation, when pressures dropped to \leq c. 0.4 GPa.

The Saualpe, the probable type-locality for "eclogite" (*sensu* Haüy, 1822), is an essential part of the so-called "eo-Alpine high-pressure belt" (EHB; see Thöni, 2006, for a review). The most interesting geochronologic aspect of this belt is the synchronism of the early exhumation history. In addition, the timing of Cretaceous andalusite formation in the western part of the EHB seems to be similar to Kienberg. Peak metamorphic garnet crystallization in the Schneeberg Complex is constrained by Sm-Nd dating between 94.1 ± 2.2 and 90.9 ± 4.1 Ma, and the Rb-Sr system in biotite closed at c. 80-75 Ma (Habler et al., 2001, and unpubl. data; Sölvä et al., 2005).

Additional evidence for a wide-spread marked pressure drop/rapid exhumation in the time window roughly between 90 and 85 Ma exists, since the 87-86 Ma Sm-Nd garnet ages from various parts of the EHB have been interpreted as documenting garnet post-pressure peak crystallization (data compilation in Thöni, 2006). These 87-86 Ma ages strongly support a synchronous decompression/exhumation of deeply buried Austroalpine basement rocks extending in E-W direction over a distance of about 400 km. For one of these localities (the Koralpe), local decompression melting was inferred (Thöni and Miller, 2000), indicating a situation similar to that described for Kienberg in the present study.

7. CONCLUSIONS

- The present study (Kienberg, central Saualpe) documents local pegmatoid melt emplacement for restricted domains of deeply subducted Austroalpine basement units; this occurred during the early stages of decompression / fast exhumation, in the course of the eo-Alpine tectonometamorphic cycle, implying local decompression melting of Ky-flasergneiss. Composition and Cretaceous age of this pegmatoid is in contrast to the numerous Permian-Triassic meta-pegmatites from the wider study area, the Saualpe-Koralpe region.

- Garnet from the Kienberg pegmatoid yielded a Sm-Nd (Grt-wr) age of 88.0 ± 1.1 Ma.

- Pegmatoid and host Grt-Ky-Bt flasergneiss show identical (crustal) Nd isotopic signatures (ϵ_{Nd} at 90 Ma = -9.4 and -9.3, respectively).

- Andalusite crystallized either as euhedral or poikiloblastic grains within the pegmatoid, or forms discordant late, pinkish veins; interpretation of this well-preserved andalusite as a pre-Cretaceous low-P relictic phase may therefore be excluded.

- Following the reconstruction of a major part of the P-T-t path from one single outcrop, andalusite crystallized in the time window $< 86 - > 80$ Ma B. P.

- Narrow magnetic splitting and careful optical mineral separation (handpicking) permit distinct age resolution even for continuously zoned minerals of complex reaction assemblages that grew over a longer time span, and using "conventional"

bulk multi-grain dating techniques (ID-TIMS).

- Tight textural and microchemical control, both in thin section (microscopy, microprobe) and of splits of the handpicked mineral separates used for isotope analysis are a must for successful dating and sound interpretation of the geochronological data.

- The present example demonstrates that garnet dating is a useful geochronological tool even for unravelling complex tectonometamorphic histories, since garnet is the only refractory major phase with significant parent-daughter fractionation for several different decay systems, and its geochronological and trace element information can be directly linked with textural/microstructural, microchemical and pressure-temperature information extracted from one and the same material.

ACKNOWLEDGEMENTS

We thank J. Mörtl for providing information about the Kienberg locality. Monika Horschinegg is thanked for performing the Rb-Sr analytical work, and Norbert Irnberger for assistance with preparation of the figures. J. Konzett and B. Fügenschuh (Innsbruck) improved the manuscript by new input and constructive criticism. This contribution profited by financial support of the Austrian Science Fund (FWF), project no. P15644-N06.

REFERENCES

- Anczkiewicz, R., Thirlwall, M.F., 2003. Improving precision of Sm-Nd garnet dating by H_2SO_4 leaching - a simple solution to the phosphate inclusion problem. Geological Society of London, Special Publications, 220, 83-91.
- Baxter, E.F., DePaolo, D.J., 2004. Can metamorphic reactions proceed faster than bulk strain? Contributions to Mineralogy and Petrology, 146, 657-670.
- Beck-Mannagetta, P., 1980. Geologische Karte der Republik Österreich 1:50.000, 188 Blatt Wolfsberg, Verlag der Geologischen Bundesanstalt Wien.
- Degeling, H.S., 2003. Zr equilibria in metamorphic rocks. PhD thesis, Australian National University, Canberra, Australia, 231 pp.
- Ferry, J.M., Watson, E.B., 2007. New thermometric models and revised calibrations for the Ti-in-zircon and Zr-in-rutile thermometers. Contributions to Mineralogy and Petrology, 154, 429-437.
- Habler, G., Linner, M., Thiede, R.C., Thöni, M., 2001. Andalusitbildung im Schneeberger Zug (SE Ötztalkristallin, Italien/Österreich). Mitteilungen der Österreichischen Mineralogischen Gesellschaft, 146, 100-102.
- Habler, G., Thöni, M., 2001. Preservation of Permo-Triassic low-pressure assemblages in the Cretaceous high-pressure metamorphic Saualpe crystalline basement (Eastern Alps, Austria). Journal of Metamorphic Geology, 19, 679-697.

- Habler, G., Thöni, M., Cotza, G., Grasemann, B., Fügenschuh, B., Sölva, H., 2007a. Polymetamorphism and deformation in the hanging wall of a Cretaceous extrusion zone (Austroalpine Ötztal Stubai basement, Eastern Alps). *Geophysical Research Abstracts*, 9, 09267 (EGU 2007).
- Habler, G., Thöni, M., Miller, C., 2007b. Major and trace element chemistry and Sm–Nd age correlation of magmatic pegmatite garnet overprinted by eclogite-facies metamorphism. *Chemical Geology*, 241, 4-22.
- Habler, G., Thöni, M., Grasemann, B., 2009. Cretaceous metamorphism in the Austroalpine Matsch Unit (Eastern Alps): The interrelation between deformation and chemical equilibrium processes. *Mineralogy and Petrology*, 97, 149-171.
- Haüy, R., 1822. *Traité de Minéralogie* (Seconde édition). Bachelier et Huzar, Paris.
- Heede, H.-U., 1997. Isotopengeologische Untersuchungen an Gesteinen des ostalpinen Saualpenkristallins, Kärnten-Österreich. *Münstersche Forschungen für Geologie und Paläontologie*, 81, 1-168.
- Hoernes, S., 1971. Petrographische Untersuchungen an Paragneisen des polymetamorphen Silvrettakristallins. *Tschermaks Mineralogische und Petrographische Mitteilungen*, 15, 56-70.
- Kleemann, U., Reinhardt, J., 1994. Garnet-biotite thermometry revisited: the effect of Al^{VI} and Ti in biotite. *European Journal of Mineralogy*, 6, 925-941.
- Koziol, A.M., Newton, R.C., 1988. Redetermination of the anorthite breakdown reaction and improvement of the plagioclase-garnet-Al₂SiO₅-quartz geobarometer. *American Mineralogist*, 73, 216-233.
- Ludwig, K.R., 2003. User's manual for Isoplot 3.00. In: *Berkeley Geochronology Center Special Publication*, 74 pp.
- Lugmair, G.W., Marti, K., 1978. Lunar initial ¹⁴³Nd/¹⁴⁴Nd: Differential evolution of the lunar crust and mantle. *Earth and Planetary Science Letters*, 39, 3349-3357.
- Manby, G.M., Thiedig, F., 1988. Petrology of eclogites from the Saualpe, Austria. *Schweizerische Mineralogische und Petrographische Mitteilungen*, 68, 441-466.
- Meixner, H., 1953. Klassische und neuere Mineralvorkommen im Eklogitbereich der Saualpe. *Carinthia II*, 143, 132-139.
- Meixner, H., 1975. Minerale und Lagerstätten im Bereich der Saualpe, Kärnten. *Clausthaler geologische Abhandlungen, Sonderband 1*, 199-217.
- Michard, P., Gurriet, P., Soudant, N., Albarède, F., 1985. Nd isotopes in French Phanerozoic shales: external vs. internal aspects of crustal evolution. *Geochimica et Cosmochimica Acta*, 49, 601-610.
- Miller, C.F., Stoddard, E.F., 1981. The role of manganese in the paragenesis of magmatic garnet: an example from the Old Woman-Piute range, California. *Journal of Geology*, 89, 233-246.
- Miller, C., Thöni, M., Konzett, J., Kurz, W., Schuster, R., 2005. Eclogites from the Koralpe and Saualpe type-localities, Eastern Alps, Austria. *Mitteilungen der Österreichischen Mineralogischen Gesellschaft*, 150, 227-263.
- Morauf, W., 1981. Rb-Sr- und K-Ar-Isotopenalter an Pegmatiten aus Kor- und Saualpe, SE-Ostalpen, Österreich. *Tschermaks Mineralogische und Petrographische Mitteilungen*, 28, 113-129.
- Mörtl, J. Die Verbreitung der Aluminiumsilikate Andalusit, Sillimanit und Kyanit (Disthen) im ostalpinen Kristallin Kärntens. *Naturwissenschaftlicher Verein für Kärnten, Austria*, 231-244, download unter www.biologiezentrum.at
- Pollington, D., Baxter, E.F., 2010. High resolution Sm-Nd garnet geochronology reveals the uneven pace of tectonometamorphic processes. *Earth and Planetary Science Letters*, 293, 63-71.
- Purtscheller, F., 1969. Petrographische Untersuchungen an Alumosilikatgneisen des Ötztaler-Stubai Altkristallins. *Tschermaks Mineralogische und Petrographische Mitteilungen*, 13, 35-54.
- Schmid, S.M., Fügenschuh, B., Kissling, E., Schuster, R., 2004. Tectonic map and overall architecture of the Alpine orogen. *Eclogae Geologicae Helveticae*, 97, 93-117.
- Schuster, R., Scharbert, S., Abart, R., Frank, W., 2001. Permo-Triassic extension and related HT/LP metamorphism in the Austroalpine – Southalpine realm. *Mitteilungen der Gesellschaft der Geologie- und Bergbaustudenten Österreichs*, 45, 111-141.
- Schuster, R., Stüwe, K., 2008. Permian metamorphic event in the Alps. *Geology*, 36, 603-606.
- Schweigl, J., 1995. Neue geochronologische und isotopengeologische Daten zur voralpidischen Entwicklungsgeschichte im Ötztalkristallin (Ostalpen). *Jahrbuch der Geologischen Bundesanstalt*, 138, 131-149.
- Sölva, H., Grasemann, B., Thöni, M., Thiede, R.C., Habler, G., 2005. The Schneeberg Normal Fault Zone: Normal faulting associated with Cretaceous SE-directed extrusion in the Eastern Alps (Italy/Austria). *Tectonophysics*, 401, 143-166.
- Steiger, R., Jäger, E., 1977. Subcommission on Geochronology: Convention on the use of decay constants in geo- and cosmochronology. *Earth and Planetary Science Letters*, 36, 359-362.

- Thöni, M., 2002. Sm-Nd isotope systematics in garnet from different lithologies (Eastern Alps): age results, and an evaluation of potential problems for Sm-Nd garnet chronometry. *Chemical Geology*, 185, 255-281.
- Thöni, M., 2006. Dating eclogite-facies metamorphism in the Eastern Alps – approaches, results, interpretations: a review. *Mineralogy and Petrology*, 88, 123-148.
- Thöni, M., Jagoutz, E., 1992. Some new aspects of dating eclogites in orogenic belts: Sm-Nd, Rb-Sr, and Pb-Pb isotopic results from the Austroalpine Saualpe and Koralpe type-locality (Carinthia/Styria, southeastern Austria). *Geochimica et Cosmochimica Acta*, 56, 347-368.
- Thöni, M., Miller, C., 1996. Garnet Sm-Nd data from the Saualpe and the Koralpe (Eastern Alps, Austria): chronological and PT constraints on the thermal and tectonic history. *Journal of Metamorphic Geology*, 14, 453-466.
- Thöni, M., Miller, C., 2000. Permo-Triassic pegmatites in the eo-Alpine eclogite-facies Koralpe complex, Austria: age and magma source constraints from mineral chemical, Rb-Sr and Sm-Nd isotope data. *Schweizer Mineralogische und Petrographische Mitteilungen*, 80/2, 169-186.
- Thöni, M., Miller, C., Blichert-Toft, J., Whitehouse, M.J., Konzett, J., Zanetti, A., 2008a. Timing of high-pressure metamorphism and exhumation of the eclogite type-locality (Kupferbrunn-Prickler Halt, Saualpe, south-eastern Austria): constraints from correlations of the Sm-Nd, Lu-Hf, U-Pb and Rb-Sr isotopic systems. *Journal of Metamorphic Geology*, 26, 561-581.
- Thöni, M., Miller, C., Zanetti, A., Habler, G., Goessler, W., 2008b. Sm-Nd isotope systematics of high-REE accessory minerals and major phases: ID-TIMS, LA-ICP-MS and EPMA data constrain multiple Permian-Triassic pegmatite emplacement in the Koralpe, Eastern Alps. *Chemical Geology*, 254, 216-237.
- Thöni, M., Miller, C., 2009. The "Permian event" in the Eastern Alps: Sm-Nd and P-T data recorded by multi-stage garnet from the Plankogel unit. *Chemical Geology*, 260, 20-36.
- Tomkins, H.S., Powell, R., Ellis, D.J., 2007. The pressure dependence of the zirconium-in-rutile thermometer. *Journal of Metamorphic Geology*, 25, 703-713.
- Tracy, R.J., Robinson, P., Thompson, A.B., 1976. Garnet composition and zoning in the determination of temperature and pressure of metamorphism, central Massachusetts. *American Mineralogist*, 61, 762-775.
- Troitzsch, U., Ellis, D.J., 2004. High-PT study of solid solutions in the system ZrO_2 - TiO_2 : the stability of srilankite. *European Journal of Mineralogy*, 16, 577-584.
- Tropper, P., Hoinkes, G., 1996. Geothermobarometry of Al_2SiO_5 -bearing metapelites in the western Austroalpine Ötztal basement. *Mineralogy and Petrology*, 58, 145-170.
- Watson, E.B., Wark, D.A., Thomas, J.B., 2006. Crystallization thermometers for zircon and rutile. *Contributions to Mineralogy and Petrology*, 151, 413-433.
- Wiesinger, M., Neubauer, F., Handler, R., 2006. Exhumation of the Saualpe eclogite unit, Eastern Alps: constraints from $^{40}Ar/^{39}Ar$ ages and structural investigations. *Mineralogy and Petrology*, 88, 149-180.
- Yardley, B.W.D., 1977. An empirical study of diffusion in garnet. *American Mineralogist*, 62, 793-800.
- Zack, T., Moraes, R., Kronz, A., 2004a. Temperature dependence of Zr in rutile: an empirical calibration of a rutile thermometer. *Contributions to Mineralogy and Petrology*, 148, 471-488.
- Zack, T., von Eynatten, H., Kronz, A., 2004b. Rutile geochemistry and its potential use in quantitative provenance studies. *Sedimentary Geology*, 171, 37-58.

Received: 25 January 2010

Accepted: 15 October 2010

Martin THÖNI¹⁾ & Christine MILLER²⁾

¹⁾ Department für Lithosphärenforschung, Universität Wien, Althanstrasse 14, A-1090 Vienna, Austria;

²⁾ Institut für Mineralogie und Petrographie, Universität Innsbruck, Innrain 52, A-6020 Innsbruck, Austria;

³⁾ Corresponding author, martin.thoeni@univie.ac.at